Altered Upper Airway and Soft Tissue Structures in the New Zealand Obese Mouse

Michael J. Brennick, Allan I. Pack, Kei Ko, Eugene Kim, Stephen Pickup, Greg Maislin and Richard J. Schwab

ONLINE DATA SUPPLEMENT

On-line supplement:

Figure E1 is an example of two NZO mice sleeping upright. Such images suggest that the NZO mouse has a compromised upper airway. “QuickTime” ®Apple Software viewable movies of the upper airway (see Movie E1) and total mouse (see Movie E2) can be viewed at the following website (www.atsjournals.org). These movies highlight in 3D the enlargement of the volume of the upper airway structures and demonstrated the increased volume of subcutaneous and visceral fat in the NZO compared to the NZW mice. Table E1 shows the 26 variables measured in this investigation by domain with means and standard deviation (SD) for each. Table E2 demonstrates the rank order false-discovery rate p-values for all of the 26 measurements.

The dynamic behavior of the mouse pharynx at matched loci (in the hypopharyngeal region) is shown in two QuickTime movies, NZW Pharynx in Breathing and NZO pharynx in breathing (Movie E3 and Movie E4, respectively). In Movie E3 the airway is reduced in size during inspiration (first image only), and then enlarges in expiration (following 5 images). In Movie E4, the airway is dilated in inspiration (first two images), and then becomes smaller during expiration (following 4 images).

Image Analysis:

The fat weighted images were displayed using Vida software on a 0-254 scale (with 2 bytes reserved for masking). The Dixon fat weighted images are not strictly black or white but show a gradient of white grey to black intensities and this is due to the relative type and concentration of fat in the image. The analysis of fat in the fat weighted axial images was determined by a threshold method such that for a single series, a value that corresponded to maximum intensity and minimum intensity were used. These values were determined by

changing the image intensity on the VIDA scale value while observing (1) when the oil phantom was brightest (maximum value), and (2) observing when the oil phantom intensity disappeared (minimum value). A combination of proton weighted and fat weighted MR images were analyzed such that the fat oil phantom was used as the thresholding standard, but in some cases (where the phantom was not adequately imaged) the subcutaneous fat of the mouse was used as the standard to threshold visceral fat in the same image. Regions of interest were manually drawn in the head and neck images representing the boundaries of each of the following structures; tongue, soft palate, parapharyngeal fat, lateral pharyngeal walls, masseter, mandible and airway.

Validation Studies of Upper Airway Measurements

We performed a validation analysis on the upper airway structures (volume of the masseter, soft palate, tongue, lateral pharyngeal walls, and parapharyngeal fat pads as well as width of the mandible to ensure that our data analysis techniques were reproducible (Table E3). The coefficient of variation (standard deviation divided by the mean) was used to assess reproducibility of each measure for one NZO animal and one NZW animal based on 3 independent replications of the measurements by one technician (one scan was obtained on each animal and the analysis was performed 3 times by one technician). For the NZO mouse, the coefficient of variation's ranged from 2.5% to 4.2% for the three replications. For the NZW, the coefficient of variation's ranged from 0.9% to 6.8% for the three replications (see Table E3). Thus, the upper airway analysis techniques used in this study resulted in highly reproducible measurements.

Determination of Upper Airway and Abdominal Structures

The mouse upper airway and surrounding anatomy has never been carefully defined using MRI. Therefore, below we illustrate how we segmented each of the upper airway

structures. Figures E2 and E3 highlight the mid-sagittal and axial images of the NZW mouse in general. Segmentation of the upper airway structures is displayed for the soft palate in Figures (E4, E5), lateral pharyngeal walls (E6, E7), parapharyngeal fat pads (E8, E9), tongue (E10, E11), mandible (E12, E13), airway (E14-E15). In addition we show how we determined subcutaneous and visceral fat measurements in the 4 anatomic regions of a NZO mouse: neck (E16, E17), thorax (E18, E19), upper abdomen (E20, E21) and lower abdomen (E22, E23).

Neck Region:

The neck region (Figure E16 denotes the span of the neck region, enclosed by orange lines, on a mid-sagittal image of a NZO mouse) was defined from the first appearance of the tympanic bulla (Figure E17A) to of the appearance of the lungs. The dotted line in Figure E16 demonstrates the location of the axial slice in Figure E17A.

Thoracic Region:

The proximal margin of the thoracic region is defined by the beginning of the lungs and the distal margin is defined by the disappearance of the lungs. The mid-sagittal image (Figure E18) of a NZO mouse shows the proximal and distal margins of the thoracic region (orange lines). The dotted line in Figure E18 demonstrates the location of the axial slice in Figure E19.

Upper Abdominal Region:

The upper abdominal region is defined from the end of the lungs to the distal margin of the kidneys (Figure E20 denotes the beginning and end of the upper abdominal region). The dotted line in Figure E20 demonstrates the location of the axial slice in Figure E21.

Lower Abdominal Region:

The lower abdominal region is defined from the distal margin of the kidney to the first slice first showing the tail of the mouse. Figure E22 denotes the beginning and end of the upper

abdominal region. The dotted line in Figure E22 demonstrates the location of the axial slice in Figure E23.

On-line Figure Legends

Figure E1. Picture of two NZO mice sleeping upright in the corner of their cages.

Figure E2. Mid-sagittal MR image of a NZW mouse demonstrating standard anatomy. Dotted line indicates the slice that the axial MR image (Figure E3) was captured. White line = 10 mm.

Figure E3. Axial MR image of a NZW mouse demonstrating primary upper airway anatomical structures. White line = 10 mm. All axial images are shown from the original mouse supine orientation, thus the brain (dorsal) is at the bottom of the image and the tongue (ventral) is at the top of the image.

Figure E4. Mid-sagittal MR image of a NZW mouse demonstrating the rostral and caudal margins of the soft palate (solid lines) in relation to the upper airway structures. The soft palate is the bright structure dorsal (towards the brain) to the tongue. The dotted line demonstrates the location of the axial slice in Figures E5A and E5B. White line = 10 mm.

Figure E5. E5 is an axial MR image of a NZW mouse demonstrating the soft palate, as it would be segmented in a representative axial slice. Tissue characteristics of the soft palate give it a high contrast (white intensity) in the proton density MR images. White line = 10 mm.

Figure E6. Mid-sagittal MR image of a NZW mouse demonstrating the rostral and caudal margins of the lateral pharyngeal walls (solid lines) in relation to the upper airway structures. The dotted line demonstrates the location of the axial slice in Figures E7A and E7B. White line = 10 mm.

Figure E7. E7A is an axial MR image of a NZW mouse demonstrating the lateral pharyngeal walls unsegmented and Figure E7B shows the segmented lateral pharyngeal walls (white). The lateral wall is bordered anteriorly by the mandible and tongue, laterally bordered by the

mandible, medially by the tongue and the posteriorly (dorsally) by the brain. White line = 10 mm.

Figure E8. Mid-sagittal MR image of a NZW mouse demonstrating the rostral and caudal margins of the parapharyngeal fat pads (solid lines) in relation to the upper airway structures. The dotted line demonstrates the location of the axial slice in Figure E9. White line = 10 mm.

Figure E9. An axial MR image of a NZW mouse demonstrating the location of the parapharyngeal fat pads (left fat pad segmented, seen as white, the right fat pad unsegmented). White line = 10 mm.

Figure E10. Mid-sagittal MR image of a NZW mouse demonstrating the rostral and caudal margins of the tongue (solid lines) in relation to the upper airway structures. The dotted line demonstrates the location of the axial slices in Figure E11A and E11B. White line = 10 mm.

Figure E11. E11A is an axial MR image of a NZW mouse demonstrating the tongue unsegmented and Figure E11B shows the segmented tongue (white). White line = 10 mm.

Figure E12. Mid-sagittal MR image of a NZW mouse demonstrating the rostral and caudal margins of the mandible (solid lines) in relation to the upper airway structures. Bone is black on this spin-echo proton density MRI. The dotted line demonstrates the location of the axial slice in Figure E13. White line = 10 mm.

Figure E13. An axial MR image of a NZW mouse demonstrating the distance between the mandibular rami. White line = 10 mm.

Figure E14. Mid-sagittal MR image of a NZW mouse demonstrating the rostral and caudal margins of the upper airway (solid lines) in relation to the upper airway structures. The dotted line demonstrates the location of the axial slices in Figure E15A and E15B. White line = 10 mm.

Figure E15. E15A is an axial MR image of a NZW mouse demonstrating the upper airway caliber unsegmented and Figure E15B shows the airway segmented (white). White line = 10 mm.

Figure E16. Mid-sagittal MR image of a NZO mouse demonstrating the rostral and caudal margins of the neck region (solid lines). The neck region was defined from the first appearance of the tympanic bulla (Figure 17A) to the appearance of the lungs. The dotted line demonstrates the location of the axial slices in Figure E17A.

Figure E17. E17A is an axial MR image of a NZO mouse demonstrating the tympanic bulla and Figure E17B shows subcutaneous fat (white) in the neck.

Figure E18. Mid-sagittal MR image of a NZO mouse demonstrating the rostral and caudal margins of the thoracic region (solid lines). The lungs are filled with fluid since this mouse was imaged after being euthanized. The proximal margin of the thoracic region is defined by the beginning of the lungs and the distal margin is defined by the disappearance of the lungs (at the level of the diaphragm). The dotted line demonstrates the location of the axial slice in Figure E19.

Figure E19. An axial MR image of a NZO mouse in thoracic region demonstrating subcutaneous and visceral fat (white) in the thorax. Again, blood pooling and fluid fills part of the lungs since this mouse was imaged after being euthanized.

Figure E20. Mid-sagittal MR image of a NZO mouse demonstrating the rostral and caudal margins of the upper abdominal region (solid lines). The lungs in the sagittal image are filled with fluid since this mouse was imaged after being euthanized. The upper abdominal region is defined from the end of the lungs to the distal margin of the kidneys. The dotted line in Figure E20 demonstrates the location of the axial slice in Figure E21. Note the location of the visceral fat.

Figure E21. An axial MR image of a NZO mouse in upper abdominal region demonstrating subcutaneous and visceral fat (white) and the kidneys.

Figure E22. Mid-sagittal MR image of a NZO mouse demonstrating the rostral and caudal margins of the lower abdominal region (solid lines). The lungs are filled with fluid since this mouse was imaged after being euthanized. The lower abdominal region is defined from the distal margin of the kidney to the first slice first showing the tail of the mouse. The dotted line in Figure E22 demonstrates the location of the axial slice in Figure E23. Note the location of the visceral fat.

Figure E23. An axial MR image of a NZO mouse in lower abdominal region demonstrating subcutaneous and visceral fat (white) and the intestines. The unusual shape of the axial image is due to the lower abdominal position that was partially contained in a rigid plastic holder (lower portion) while the upper body freely flowed over the plastic supporting holder.

Table E1 Variables Measured by Domain: Mean Results ± SD for NZW and NWO mice

	NZO Means ± SD	NZW Means ± SD
General		
Age (weeks)	21.6 ± 5.85	23.1 ± 5.82
Weight (g)	54.1 ± 7.19	35.7 ± 1.86
Respiratory Rate (breaths/min)	73.1 ± 12	69.1 ± 10.9
Upper Airway Structures		
Masseter (volume)	215 ± 33.01	203 ± 31
Soft Palate (volume)	5.86 ± 1.28	4.64 ± 0.88
Tongue (volume)	137 ± 25.96	104 ± 18
Lateral Walls (volume)	111 ± 26.9	84.5 ± 16.2
Fat Pads (volume)	5 ± 1.37	1.43 ± 0.5
Mandibular Width	7.85 ± 0.37	7.9 ± 0.34
Anterior-Posterior Distance (Airway to Back of Head, mm)	5.46 ± 0.34	5.2 ± 0.22
Neck Region		
Total Neck Fat (volume)	1940 ± 554	656 ± 385
Total Neck Tissue (volume)	5470 ± 444	3730 ± 841
% of Neck Fat/Neck Tissue	0.36 ± 0.1	0.17 ± 0.08
Thoracic Region		
Total Thoracic Fat (volume)	4260 ± 843	1293 ± 512
Total Thoracic Tissue (volume)	8440 ± 1430	5750 ± 1000
% of Thoracic Fat/Thoracic Tissue	0.5 ± 0.03	0.23 ± 0.09
Upper Abdominal Region		
Upper Abdominal Intra Fat (volume)	3570 ± 752	1010 ± 484
Upper Abdominal Subcutaneous Fat (volume)	1250 ± 528	426 ± 274
Upper Abdominal Total Fat (volume)	4820 ± 1230	1440 ± 740
Upper Abdominal Total Tissue (volume)	11700 ± 3470	7130 ± 2130
% of Upper Abdominal Fat/Abdominal Tissue	0.43 ± 0.09	0.21 ± 0.11
Lower Abdominal Region		
Lower Abdominal Intra Fat (volume)	3550 ± 844	1700 ± 785
Lower Abdominal Subcutaneous Fat (volume)	4230 ± 840	1960 ± 990
Lower Abdominal Total Fat (volume)	7780 ± 1600	3660 ± 1720
Lower Abdominal Total Tissue (volume)	13400 ± 2170	9730 ± 1500
% of Lower Abdominal Fat/Lower Tissue	0.58 ± 0.04	0.37 ± 0.15

Table E2 -Variables Rank Ordered by False Discovery Rate

False Discovery Rate < 0.0254 (Significant Variables Group)

Variable	Nominal p value	False Discovery Rate
Total Thoracic Fat	<.0001	<.0001
Weight	<.0001	<.0001
Fat Pads	<.0001	<.0001
Upper Abdominal Intra Fat	<.0001	<.0001
% of Thoracic Fat/Thoracic Tissue	<.0001	<.0001
Upper Abdominal Total Fat	<.0001	<.0001
Total Neck Fat	<.0001	<.0001
Lower Abdominal Total Fat	0.0001	0.0003
Total Neck Tissue	0.0001	0.0003
Lower Abdominal Subcutaneous Fat	0.0001	0.0003
Lower Abdominal Intra Fat	0.0002	0.0005
Total Thoracic Tissue	0.0002	0.0005
% of Neck Fat/Neck Tissue	0.0004	0.0008
Upper Abdominal Subcutaneous Fat	0.0005	0.0009
% of Upper Abdominal Fat/Abdominal Tissue	0.0005	0.0009
Lower Abdominal Total Tissue	0.0006	0.0009
% of Lower Abdominal Fat/Lower Tissue	0.0031	0.0045
Upper Abdominal Total Tissue	0.0031	0.0045
Tongue	0.0033	0.0045
Lateral Walls	0.0136	0.0177
Soft Palate	0.0207	0.0256

False Discovery Rate > 0.05 (Non-significant Variables Group)

Variable	Nominal p value	False Discovery Rate
Anterior-Posterior Distance (Airway to Back of Head)	0.0501	0.0592
Masseter	0.4026	0.4551
Respiratory Rate	0.4931	0.5342
Age	0.5907	0.6143
Mandibular Width	0.7629	0.7629

Table E3 - Reproducibility of Pharyngeal Structural Measurements.
All volume values (mm^3) except mandibular width (mm)

NZO	Replication 1	Replication #2	Replication #3	Coefficient of Variation (%)
Masseter	195.44	205.87	189.51	4.21
Soft Palate	7.17	7.77	7.46	4.02
Tongue	183.7	192.47	190.79	2.46
Lateral Walls	146.46	156.54	152.41	3.34
Parapharyngeal Fat Pads	8.65	8.74	8.02	4.63
Mandibular width (mm)	7.99	8.57	8.32	3.51

NZW	Replication 1	Replication #2	Replication #3	Coefficient of Variation (%)
Masseter	192.13	213.38	202.15	5.25
Soft Palate	5.03	4.95	4.89	1.42
Tongue	99.55	98.48	97.88	0.86
Lateral Walls	99.33	92.74	96.32	3.43
Parapharyngeal Fat Pads	0.89	0.97	0.85	6.76
Mandibular width (mm)	7.40	7.16	7.14	2.00

Figure E1

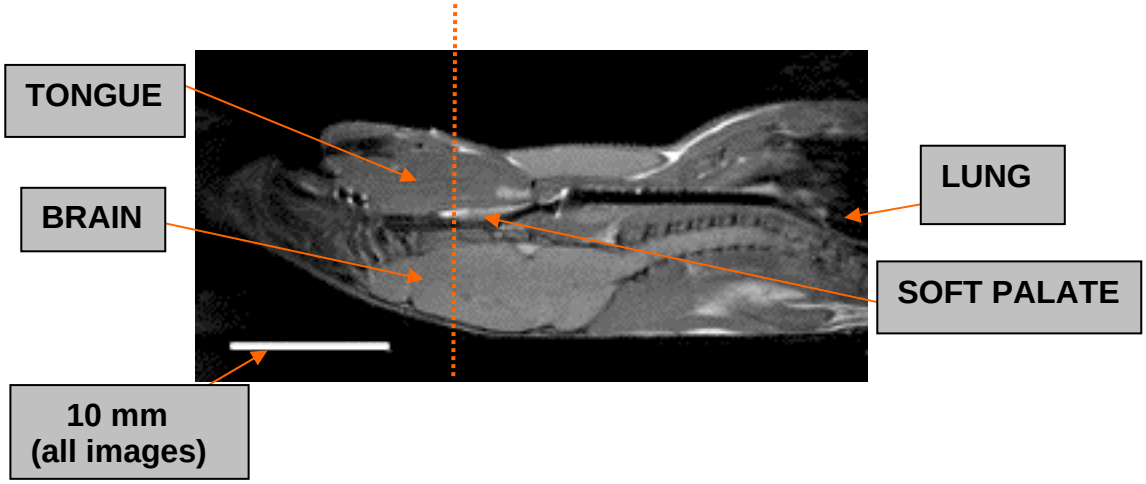

Figure E2

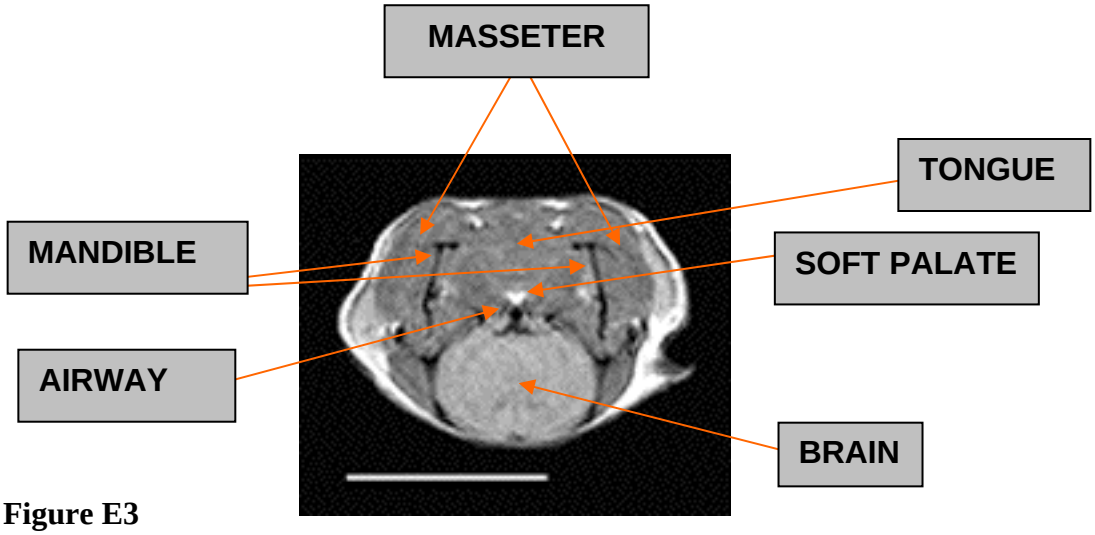

Figure E3

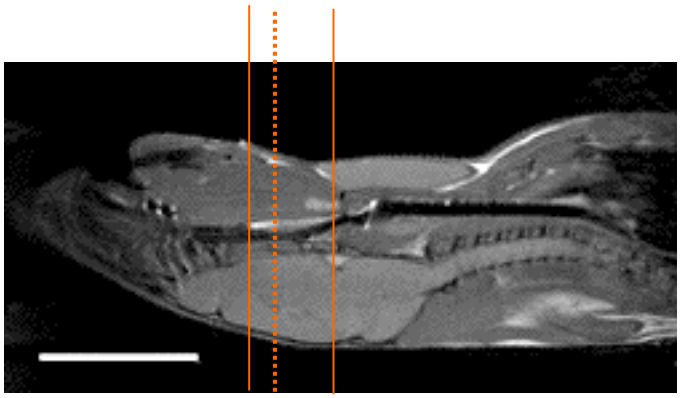

Figure E4

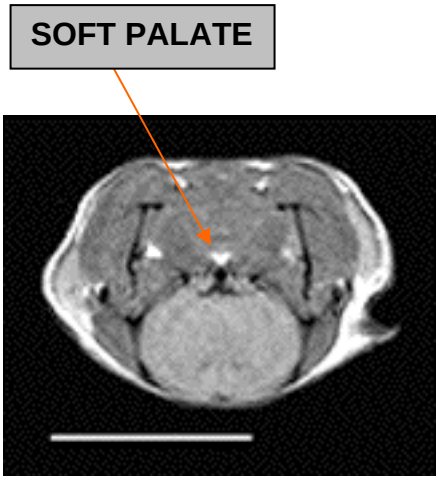

Figure E5

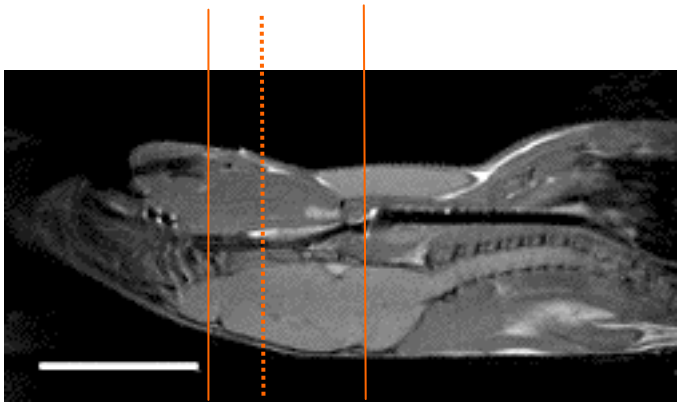

Figure E6

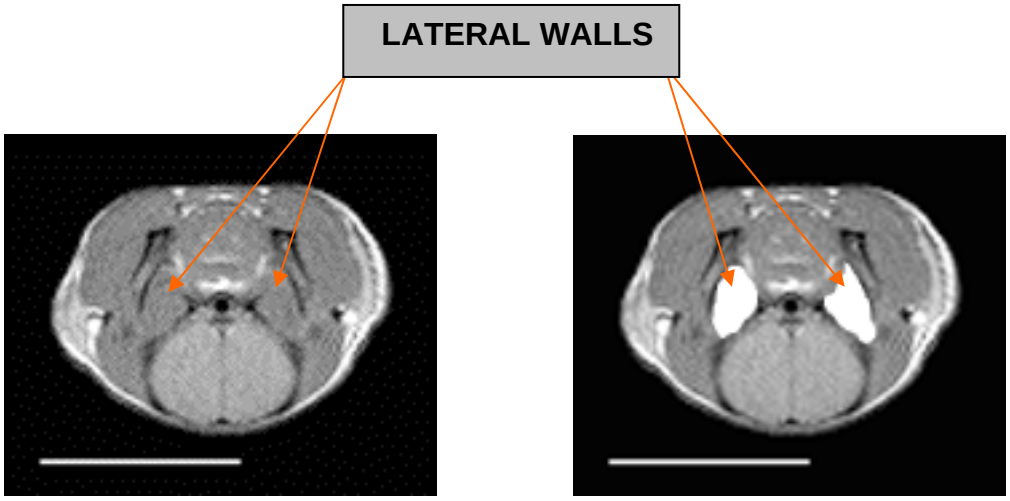

Figure E7A **Figure E7B**

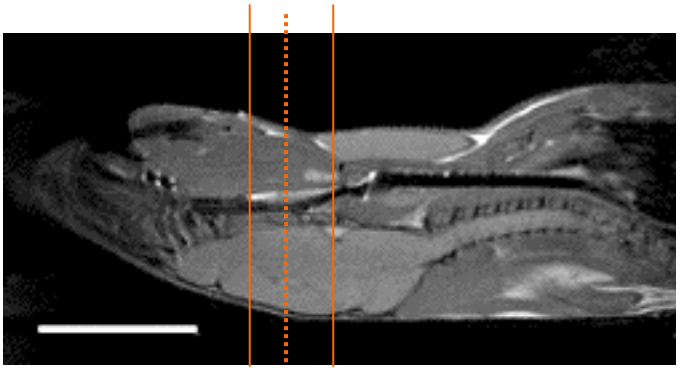

Figure E8

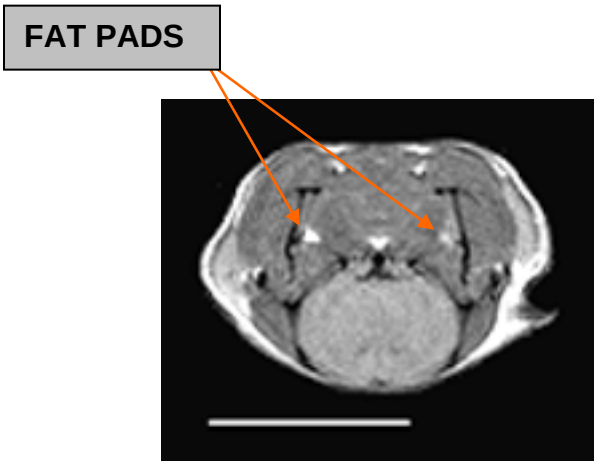

Figure E9

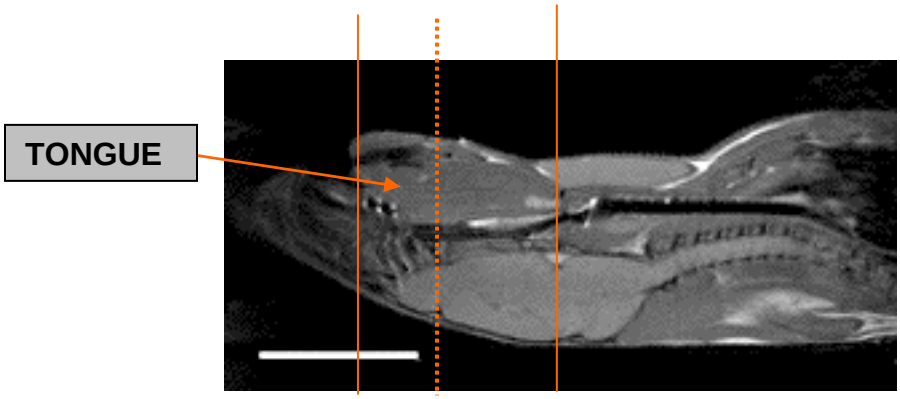

Figure E10

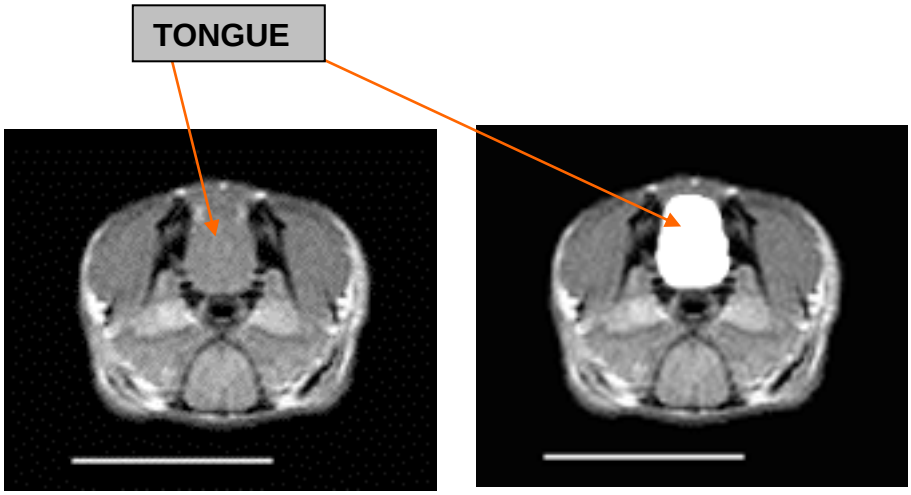

Figure E11A **Figure E11B**

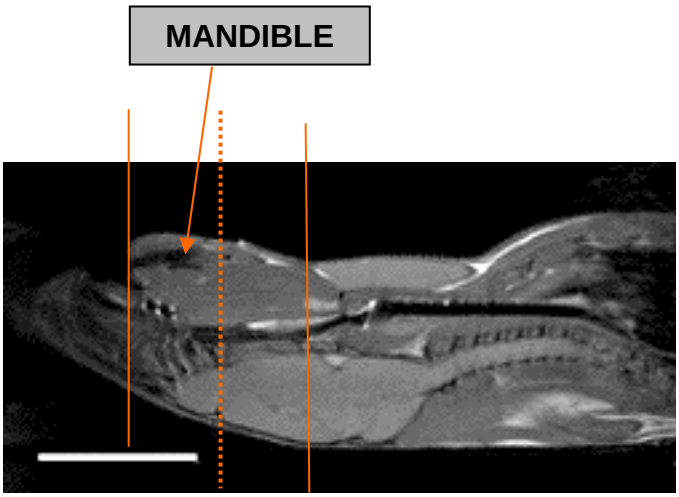

Figure E12

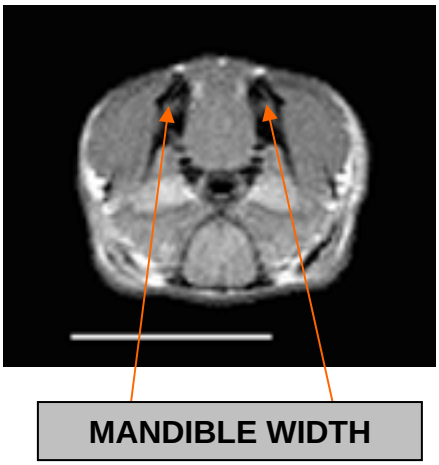

Figure E13

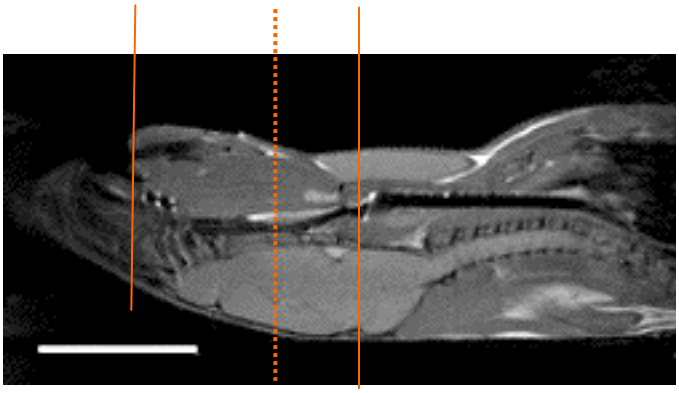

Figure E14

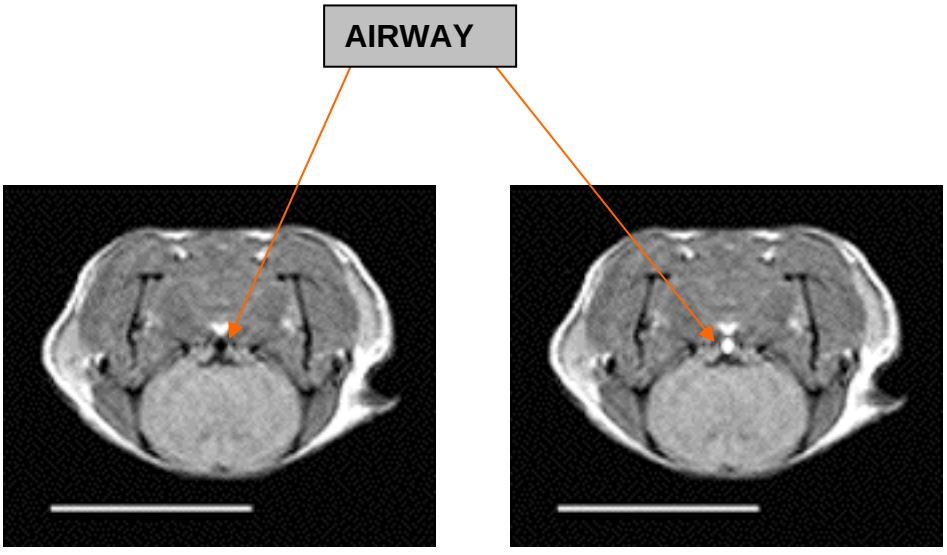

Figure E15A **Figure E15B**

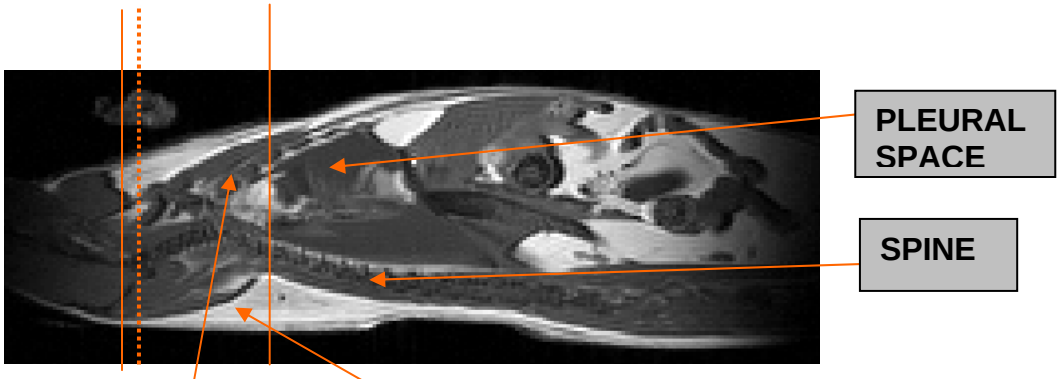

Figure E16

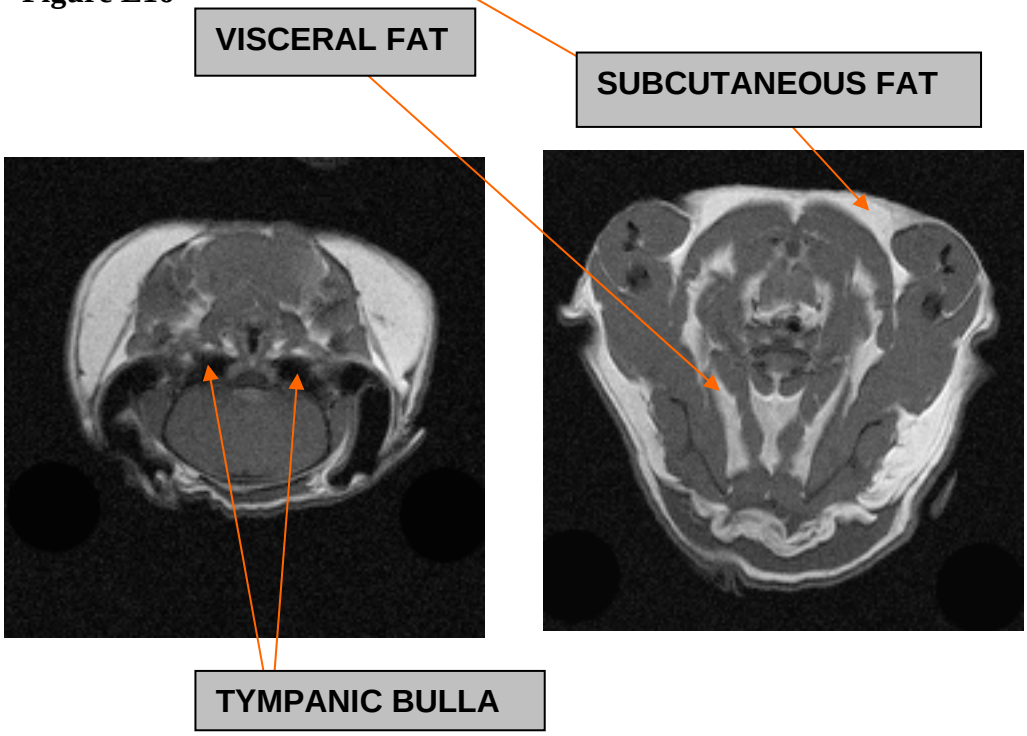

Figure E17A **Figure E17B**

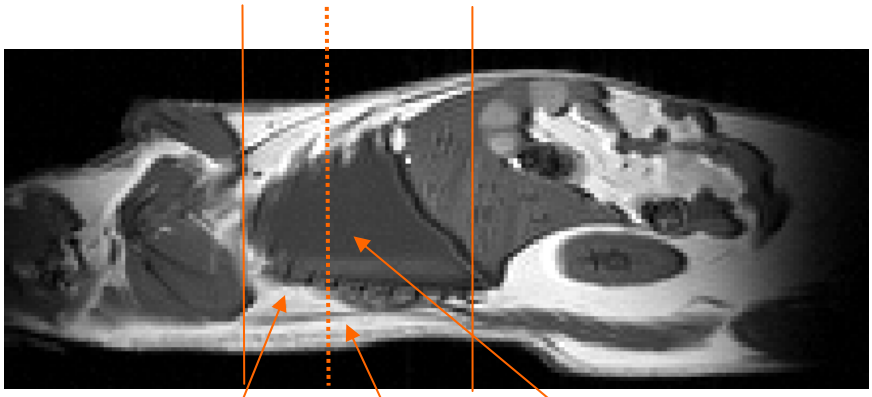

Figure E18

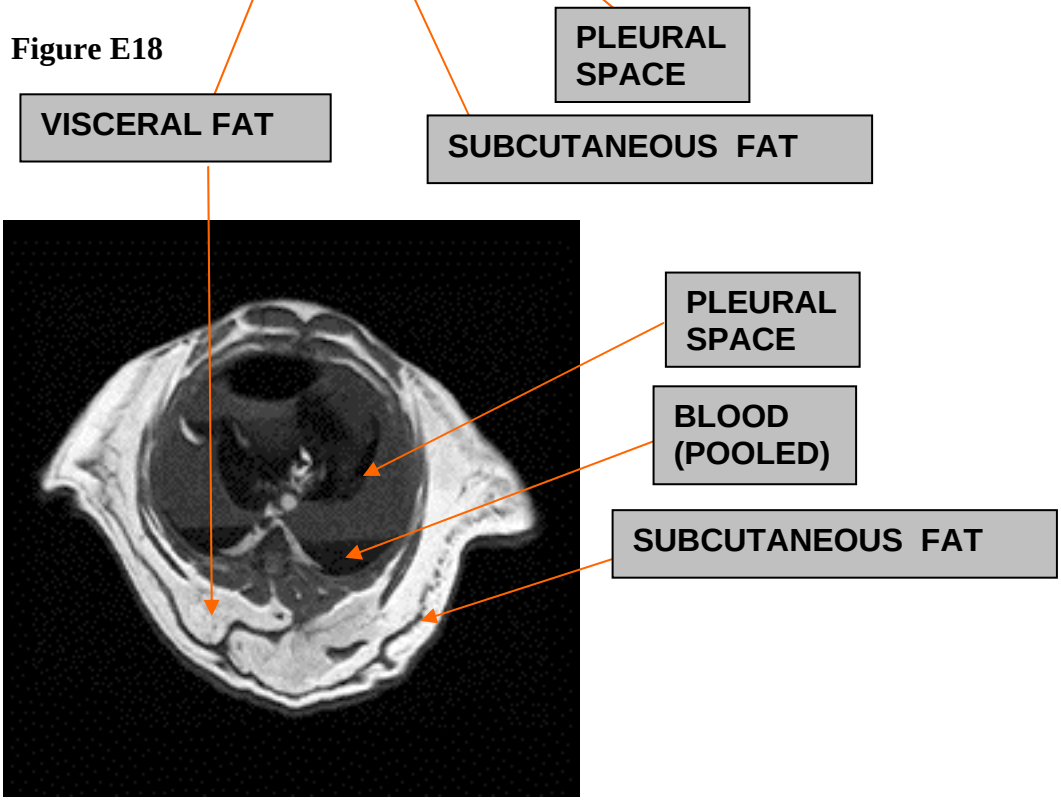

Figure E19

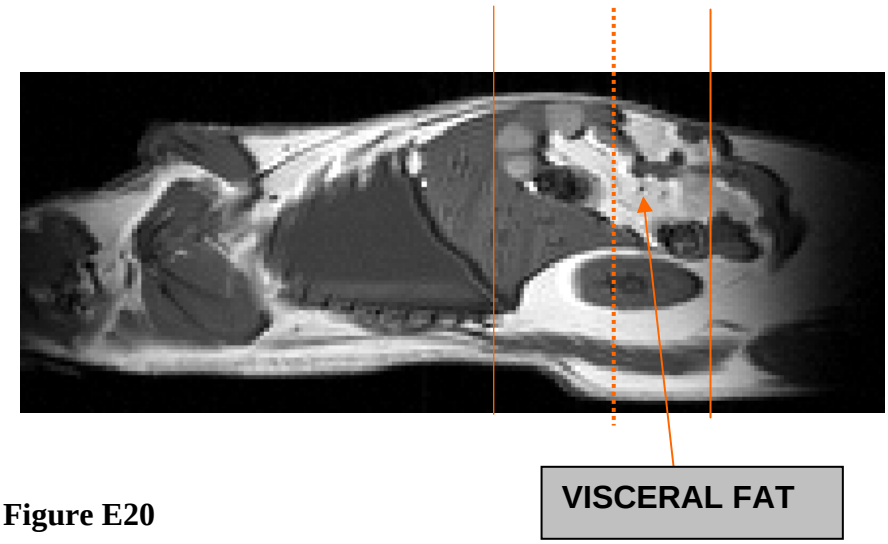

Figure E20

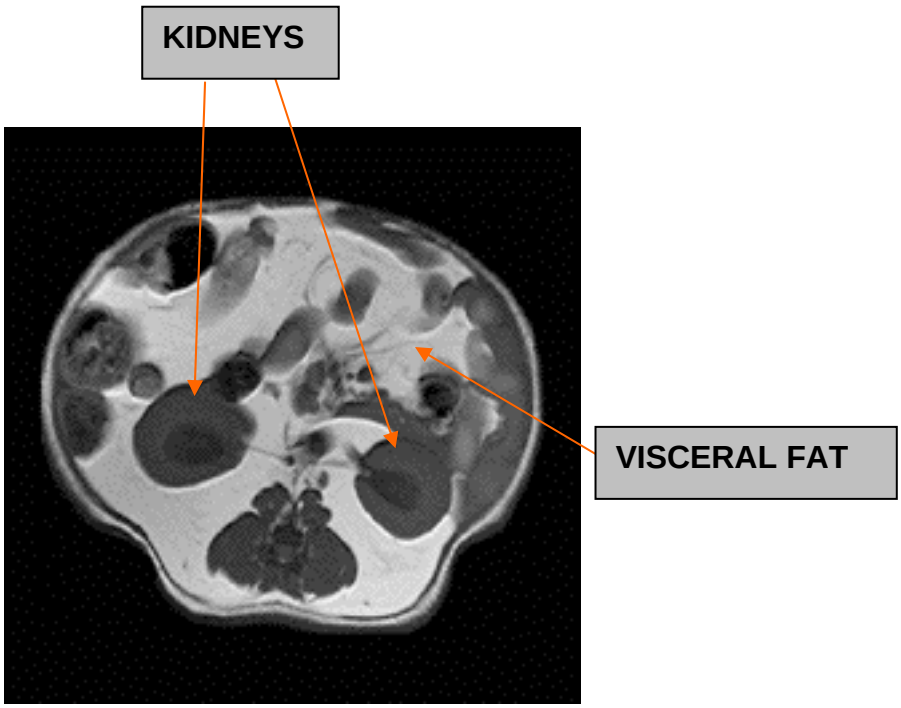

Figure E21

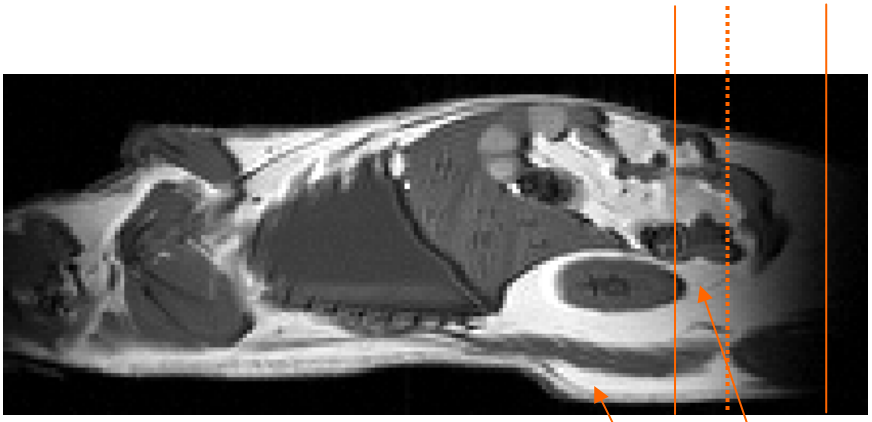

Figure E22

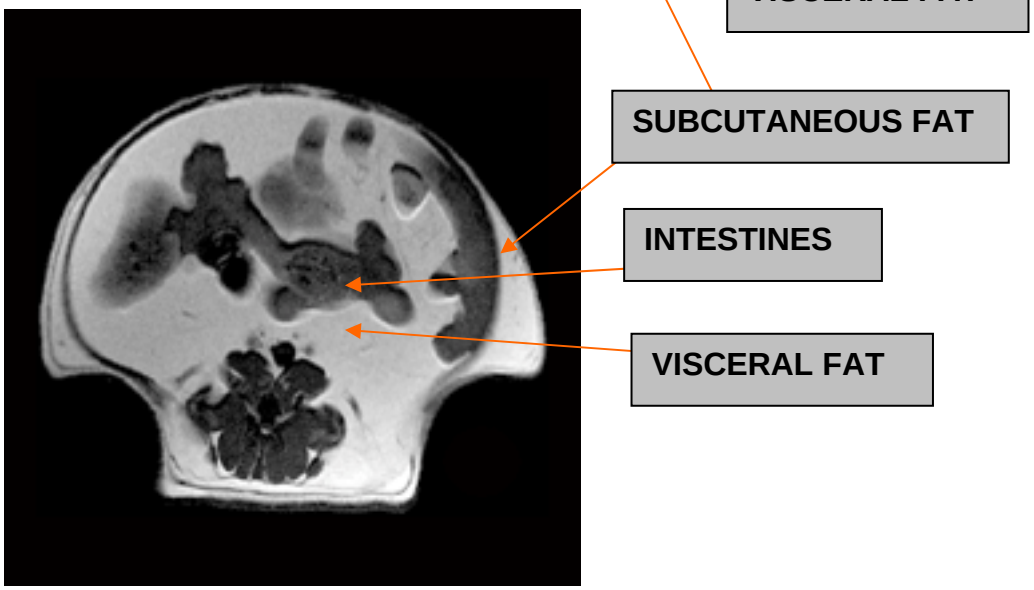

Figure E23